

Energy-Efficient D2D Underlaid MIMO Cellular Networks with Energy Harvesting

Chi-Han Lee^{*†}, Ronald Y. Chang[†], Chun-Tao Lin[‡], and Shin-Ming Cheng^{*†}

^{*}Department of Computer Science and Information Engineering,

National Taiwan University of Science and Technology, Taipei, Taiwan

[†]Research Center for Information Technology Innovation, Academia Sinica, Taipei, Taiwan

[‡]Department of Electrical Engineering, National Taipei University of Technology, Taipei, Taiwan

d10202006@mail.ntust.edu.tw, rchang@citi.sinica.edu.tw, ctl@ntut.edu.tw, smcheng@mail.ntust.edu.tw

Abstract—This paper considers the precoder design for energy-efficient data transmissions in energy harvesting (EH)-aided device-to-device (D2D) communications underlaid multiple-input multiple-output (MIMO) cellular networks. We aim to maximize the energy efficiency (EE) of the network, defined as the ratio of the system sum rate to the system power consumption, under EH and transmit power constraints for both cellular and D2D users. The considered problem is nonconvex due to the concave-convex and fractional form of the objective. We propose to apply the concave-convex procedure (CCCP) and the Dinkelbach method to find tractable, approximate solutions. Numerical results demonstrate the performance of the proposed method from various perspectives.

I. INTRODUCTION

Spectral efficiency and energy efficiency (EE) are two important performance metrics in wireless communication systems. Since device-to-device (D2D) communication [1], [2] has been shown promising in increasing the system transmission rates and spectral efficiency, it is essential to study the EE of D2D-enabled communication systems. In [3], the EE and spectral efficiency tradeoff in a D2D-enabled heterogeneous network (HetNet) was investigated. In [4], distributed resource allocation based on a game-theoretic approach was studied, where the EE of D2D-enabled cellular networks was optimized. In [5], mode switching/selection among three transmission modes for energy-efficient D2D communications in cellular networks was examined. In [6], the D2D communication underlying cellular networks was considered and the branch-and-bound algorithm was adopted to achieve energy-efficient resource allocation.

The energy harvesting (EH) technology [7], [8] enables the receivers to charge the batteries by recycling the radio frequency (RF) energy radiated from the transmitters. EH-aided D2D communication has been studied [9]–[13]. In [9], a radio resource allocation scheme that maximizes the sum-rate in EH-aided D2D communication underlying the cellular network was investigated. In [10], wireless-powered D2D communication in a time division duplex (TDD) underlying cellular network for improving the spectrum efficiency was examined.

This work was supported in part by the Ministry of Science and Technology, Taiwan, under Grants MOST 105-2628-E-011-001-MY3 and MOST 106-2628-E-001-001-MY3.

In [11], the spectral efficiency and coverage probability of EH-based D2D-assisted machine-type communications under spatially correlated interference using stochastic geometry was studied. In [12], the joint partner selection and power control problem between cellular users and D2D pairs was studied by considering EH capabilities at the cellular users. In [13], the power allocation problem and beamforming design for EH-aided D2D communications underlaid cellular networks was studied.

In multiantenna systems, the system performance can be significantly improved via the precoding (multistream beamforming) technique. In this paper, we study the *precoder design for EE maximization in D2D underlaid multiple-input multiple-output (MIMO) cellular networks with EH-enabled cellular and D2D users*, which has not been previously considered. This problem is challenging to solve due to the inherent non-convexity of concave-convex fractional programming [14]–[16]. We propose a novel design to overcome the difficulty. First, first-order Taylor approximation is applied to the convex term of the concave-convex programming (CCCP). Then, the Dinkelbach method is exploited to address the fractional form in the EE maximization. Finally, we propose to use a bisection algorithm so that the optimal precoders can be solved with convex optimization tools, e.g., CVX [17].

The outline of this paper is as follows. Sec. II introduces the system model. Sec. III presents the problem formulation. Sec. IV describes the proposed method. Sec. V presents the simulation results. Finally, conclusions are drawn in Sec. VI.

Notations: Bold lowercase and uppercase letters represent vectors and matrices, respectively. \mathbf{A}^T and \mathbf{A}^H denote standard and Hermitian transpose of \mathbf{A} , respectively. $|\mathbf{A}|$ and $\text{Tr}(\mathbf{A})$ denote the determinant and trace of \mathbf{A} , respectively. $\mathbf{A} \succeq 0$ means that \mathbf{A} is a positive semidefinite matrix. $\nabla f(\mathbf{X})$ is the gradient of $f(\mathbf{X})$. $\mathbb{C}^{m \times n}$ is the complex space of $m \times n$ matrices.

II. SYSTEM MODEL

Consider a D2D-underlaid downlink MIMO cellular network, as shown in Fig. 1. The network consists of one base station (BS), K cellular user equipments (CUEs), and L pairs of D2D user equipments (DUEs). Let N_t^C be the number

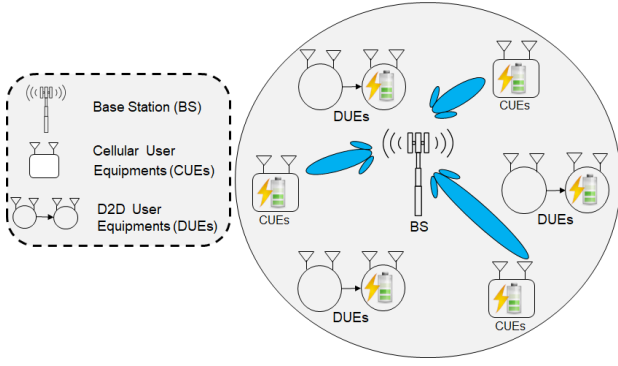


Fig. 1. A D2D-underlaid downlink MIMO cellular network with EH-enabled receivers.

of antennas at the BS, N_t^D the number of antennas at each transmitting terminal of DUE pairs, and N_r the number of antennas at each CUE and at each receiving terminal of DUE pairs. Let $\mathcal{K} = \{1, \dots, K\}$ and $\mathcal{L} = \{1, \dots, L\}$ represent the set of CUEs and DUE pairs, respectively.

A. Information Rate

Let $\mathbf{W}_k \mathbf{s}_k$ be the transmitted signal from the BS to the k th CUE, where $\mathbf{W}_k \in \mathbb{C}^{N_t^C \times m_k}$ is the linear precoder employed at the BS for the k th CUE, and $\mathbf{s}_k \in \mathbb{C}^{m_k}$ is the data symbol vector (where $\mathbb{E}[\mathbf{s}_k \mathbf{s}_k^H] = \mathbf{I}$), with m_k being the number of data streams. Let $\mathbf{x}_\ell \in \mathbb{C}^{N_t^D \times 1}$ be the transmitted signal from the transmitter to the receiver of the ℓ th DUE pair. Then, the received signal at the k th CUE is given by

$$\begin{aligned} \mathbf{y}_k^C &= \mathbf{H}_k^{\text{BS}} \sum_{i=1}^K \mathbf{W}_i \mathbf{s}_i + \sum_{\ell=1}^L \mathbf{G}_k^\ell \mathbf{x}_\ell + \mathbf{n}_k^C \\ &= \underbrace{\mathbf{H}_k^{\text{BS}} \mathbf{W}_k \mathbf{s}_k}_{\text{desired signal}} + \underbrace{\mathbf{H}_k^{\text{BS}} \sum_{i=1, i \neq k}^K \mathbf{W}_i \mathbf{s}_i}_{\text{CUE interference}} \\ &\quad + \underbrace{\sum_{\ell=1}^L \mathbf{G}_k^\ell \mathbf{x}_\ell}_{\text{DUE interference}} + \underbrace{\mathbf{n}_k^C}_{\text{noise}}, \quad k \in \mathcal{K} \end{aligned} \quad (1)$$

where $\mathbf{H}_k^{\text{BS}} \in \mathbb{C}^{N_r \times N_t^C}$ is the channel from the BS to the k th CUE, $\mathbf{G}_k^\ell \in \mathbb{C}^{N_r \times N_t^D}$ is the channel from the transmitter of the ℓ th DUE pair to the k th CUE, and $\mathbf{n}_k^C \in \mathbb{C}^{N_r \times 1} \sim \mathcal{CN}(0, \sigma_k^2 \mathbf{I})$ is the complex additive white Gaussian noise (AWGN).

Each receiving CUE/DUE has RF-EH capabilities and therefore can harvest energy from the useful signal as well as interference based on the power splitting technique [8]. The power-splitting factor for information decoding (ID) is denoted by ρ_k^C for the k th CUE and ρ_ℓ^D for the receiver of the ℓ th DUE pair (thus, the power-splitting factor for EH at the

corresponding receiver is $1 - \rho_k^C$ and $1 - \rho_\ell^D$, respectively). After power splitting, the signal for ID at the k th CUE is

$$\tilde{\mathbf{y}}_k^C = \sqrt{\rho_k^C} \mathbf{y}_k^C + \tilde{\mathbf{n}}_k^C, \quad k \in \mathcal{K} \quad (2)$$

where $\tilde{\mathbf{n}}_k^C \sim \mathcal{CN}(0, \tilde{\sigma}_k^2 \mathbf{I})$ denotes the additive noise at the ID receiver, which is independent of \mathbf{n}_k^C . Then, the sum information rate for all CUEs can be expressed as

$$\begin{aligned} R_C &= \sum_{k=1}^K \log_2 \left| \mathbf{I} + \boldsymbol{\Omega}_k^{-1} \mathbf{H}_k^{\text{BS}} \mathbf{Q}_k (\mathbf{H}_k^{\text{BS}})^H \right| \\ &= \sum_{k=1}^K \log_2 \frac{\left| \sum_{i=1}^K \mathbf{H}_k^{\text{BS}} \mathbf{Q}_i (\mathbf{H}_k^{\text{BS}})^H + \sum_{\ell=1}^L \mathbf{G}_k^\ell \mathbf{P}_\ell (\mathbf{G}_k^\ell)^H + \Phi_k^C \right|}{\left| \sum_{i \neq k}^K \mathbf{H}_k^{\text{BS}} \mathbf{Q}_i (\mathbf{H}_k^{\text{BS}})^H + \sum_{\ell=1}^L \mathbf{G}_k^\ell \mathbf{P}_\ell (\mathbf{G}_k^\ell)^H + \Phi_k^C \right|} \end{aligned} \quad (3)$$

where $\boldsymbol{\Omega}_k = \sum_{i \neq k}^K \mathbf{H}_k^{\text{BS}} \mathbf{Q}_i (\mathbf{H}_k^{\text{BS}})^H + \sum_{\ell=1}^L \mathbf{G}_k^\ell \mathbf{P}_\ell (\mathbf{G}_k^\ell)^H + \Phi_k^C$, $\mathbf{Q}_k = \mathbf{W}_k \mathbf{W}_k^H$, $\mathbf{P}_\ell = \mathbb{E}[\mathbf{x}_\ell \mathbf{x}_\ell^H]$, and $\Phi_k^C = \sigma_k^2 \mathbf{I} + \frac{\tilde{\sigma}_k^2}{\rho_k^C} \mathbf{I}$. Note that in deriving (3), we have used the properties $|\mathbf{C}\mathbf{D}| = |\mathbf{C}||\mathbf{D}|$ and $|\mathbf{C}^{-1}| = |\mathbf{C}|^{-1}$.

The information rates for DUEs can be modeled similarly. The received signal at the receiver of the ℓ th DUE pair is given by

$$\mathbf{y}_\ell^D = \sum_{j=1}^L \mathbf{H}_\ell^j \mathbf{x}_j + \mathbf{G}_\ell^{\text{BS}} \sum_{k=1}^K \mathbf{W}_k \mathbf{s}_k + \mathbf{n}_\ell^D, \quad \ell \in \mathcal{L} \quad (4)$$

where $\mathbf{H}_\ell^j \in \mathbb{C}^{N_r \times N_t^D}$ is the channel from the transmitter of the j th DUE pair to the receiver of the ℓ th DUE pair, $\mathbf{G}_\ell^{\text{BS}} \in \mathbb{C}^{N_r \times N_t^C}$ is the channel from the BS to the receiver of ℓ th DUE pair, and $\mathbf{n}_\ell^D \in \mathbb{C}^{N_r \times 1} \sim \mathcal{CN}(0, \sigma_\ell^2 \mathbf{I})$ is the complex AWGN. After power splitting, the signal for ID at the receiver of the ℓ th DUE pair is

$$\tilde{\mathbf{y}}_\ell^D = \sqrt{\rho_\ell^D} \mathbf{y}_\ell^D + \tilde{\mathbf{n}}_\ell^D, \quad \ell \in \mathcal{L} \quad (5)$$

where $\tilde{\mathbf{n}}_\ell^D \sim \mathcal{CN}(0, \tilde{\sigma}_\ell^2 \mathbf{I})$ denotes the additive noise at the ID receiver, which is independent of \mathbf{n}_ℓ^D . The sum information rate for the receivers of all DUE pairs is given by

$$\begin{aligned} R_D &= \sum_{\ell=1}^L \log_2 \frac{\left| \sum_{j=1}^L \mathbf{H}_\ell^j \mathbf{P}_j (\mathbf{H}_\ell^j)^H + \sum_{k=1}^K \mathbf{G}_\ell^{\text{BS}} \mathbf{Q}_k (\mathbf{G}_\ell^{\text{BS}})^H + \Phi_\ell^D \right|}{\left| \sum_{j \neq \ell}^L \mathbf{H}_\ell^j \mathbf{P}_j (\mathbf{H}_\ell^j)^H + \sum_{k=1}^K \mathbf{G}_\ell^{\text{BS}} \mathbf{Q}_k (\mathbf{G}_\ell^{\text{BS}})^H + \Phi_\ell^D \right|} \end{aligned} \quad (6)$$

where $\Phi_\ell^D = \sigma_\ell^2 \mathbf{I} + \frac{\tilde{\sigma}_\ell^2}{\rho_\ell^D} \mathbf{I}$.

B. Harvested Energy

The harvested energy at the k th CUE and at the receiver of the ℓ th DUE pair are given respectively by

$$\begin{aligned} E_k^C &= \mathbb{E} \left[\left\| \sqrt{\mu_k^C} \mathbf{y}_k^C \right\|^2 \right] = \mu_k^C \mathbb{E} \left[\text{Tr}(\mathbf{y}_k^C (\mathbf{y}_k^C)^H) \right] \\ &= \mu_k^C \text{Tr} \left(\sum_{i=1}^K \mathbf{H}_k^{\text{BS}} \mathbf{Q}_i (\mathbf{H}_k^{\text{BS}})^H + \sum_{\ell=1}^L \mathbf{G}_k^\ell \mathbf{P}_\ell (\mathbf{G}_k^\ell)^H + \sigma_k^2 \mathbf{I} \right), \end{aligned} \quad (7)$$

$$\begin{aligned} E_\ell^D &= \mathbb{E} \left[\left\| \sqrt{\mu_\ell^D} \mathbf{y}_\ell^D \right\|^2 \right] = \mu_\ell^D \mathbb{E} \left[\text{Tr}(\mathbf{y}_\ell^D (\mathbf{y}_\ell^D)^H) \right] \\ &= \mu_\ell^D \text{Tr} \left(\sum_{j=1}^L \mathbf{H}_\ell^j \mathbf{P}_j (\mathbf{H}_\ell^j)^H + \sum_{k=1}^K \mathbf{G}_\ell^{\text{BS}} \mathbf{Q}_k (\mathbf{G}_\ell^{\text{BS}})^H + \sigma_\ell^2 \mathbf{I} \right) \end{aligned} \quad (8)$$

where $\mu_k^C = \xi_k^C (1 - \rho_k^C)$ and $\mu_\ell^D = \xi_\ell^D (1 - \rho_\ell^D)$. ξ_k^C and ξ_ℓ^D denote energy conversion efficiency at the k th CUE and at the receiver of the ℓ th DUE pair, respectively.

C. Network Power Consumption

Here, we model the total network power consumption which includes the transmit power consumption and circuit power consumption (due to frequency conversion (up/down), digital-to-analog converter (DAC), analog-to-digital converter (ADC), mixer, filter, etc.). The total power consumption at the BS is given by

$$P_C^{\text{Total}} = \sum_{k=1}^K \text{Tr}(\mathbf{Q}_k) + P_{\text{BS}}^{\text{cir}} \quad (9)$$

where $\sum_{k=1}^K \text{Tr}(\mathbf{Q}_k)$ and $P_{\text{BS}}^{\text{cir}}$ are the transmit power and circuit power consumption at the BS, respectively. Likewise, the total power consumption at the transmitters of all DUE pairs is given by

$$P_D^{\text{Total}} = \sum_{\ell=1}^L (\text{Tr}(\mathbf{P}_\ell) + P_\ell^{\text{cir}}) \quad (10)$$

where $\text{Tr}(\mathbf{P}_\ell)$ and P_ℓ^{cir} are the transmit power and circuit power consumption at the transmitter of the ℓ th DUE pair, respectively.

III. PROBLEM FORMULATION

Our design objective is to maximize the EE, which is defined as the ratio of the system sum rate to the system total power consumption [3]–[5], [14], with harvested energy, BS transmit power, and individual D2D transmit power constraints. The power-splitting factors ρ_k^C and ρ_ℓ^D are assumed to be predetermined constants [8], [13]. Mathematically, the design problem is formulated as

$$\max_{\{\mathbf{Q}_k\}, \{\mathbf{P}_\ell\}} \frac{R_C + R_D}{P_C^{\text{Total}} + P_D^{\text{Total}}} \quad (11a)$$

$$\text{s.t.} \quad E_k^C \geq E_{\min}^C, \forall k \in \mathcal{K}, \quad (11b)$$

$$E_\ell^D \geq E_{\min}^D, \forall \ell \in \mathcal{L}, \quad (11c)$$

$$\sum_{k=1}^K \text{Tr}(\mathbf{Q}_k) \leq P_{\max}^C, \quad (11d)$$

$$\text{Tr}(\mathbf{P}_\ell) \leq P_{\max}^D, \forall \ell \in \mathcal{L}, \quad (11e)$$

$$\mathbf{Q}_k \succeq 0, \forall k \in \mathcal{K}, \quad (11f)$$

$$\mathbf{P}_\ell \succeq 0, \forall \ell \in \mathcal{L}, \quad (11g)$$

where (11b) and (11c) ensure that the harvested energy at the k th CUE and at the receiver of the ℓ th DUE pair be higher than some threshold E_{\min}^C and E_{\min}^D , respectively; (11d) and (11e) represent the BS transmit power constraint and the individual DUE transmit power constraint, respectively; (11f) and (11g) follow from the definition of \mathbf{Q}_k and \mathbf{P}_ℓ . Note that problem (11) is a nonconvex problem due to the concave-convex form in the numerator of the objective and the fractional form of the objective. It is known that the precoder design for sum-rate maximization (i.e., maximizing R_C alone, without DUEs, EH, or EE considerations) is an NP-hard problem [18], [19]. The considered problem here is more challenging since CUEs and DUEs are coupled in the objective. Thus, it is practically useful to find tractable, approximate solutions.

IV. PROPOSED ALGORITHM

We propose two efficient procedures to solve problem (11). We apply the concave-convex procedure (CCCP) [20] to the numerator of (11a) in the concave-convex form. Then, we adopt the Dinkelbach method [15], [16], [21] to deal with the nonconvex fractional form of (11a).

A. Concave-Convex Procedure (CCCP)

CCCP is based on the majorization-minimization method and is widely used in statistics, signal processing, communications, and machine learning [22]. The main concept of CCCP [20] is to iteratively linearize the convex part of the concave-convex objective function. Specifically, for R_C , we perform the first-order approximation to the logarithm of the denominator of (3) at each iteration, i.e.,

$$\begin{aligned} R_C &\approx \sum_{k=1}^K \log_2 \left| \sum_{i=1}^K \mathbf{H}_k^{\text{BS}} \mathbf{Q}_i (\mathbf{H}_k^{\text{BS}})^H + \sum_{\ell=1}^L \mathbf{G}_k^\ell \mathbf{P}_\ell (\mathbf{G}_k^\ell)^H + \Phi_k^C \right| - \\ &\sum_{k=1}^K \left(\log_2 |\boldsymbol{\Omega}_k^{(t)}| + \frac{1}{\ln(2)} \text{Tr} \left[(\boldsymbol{\Omega}_k^{(t)})^{-1} (\boldsymbol{\Omega}_k - \boldsymbol{\Omega}_k^{(t)}) \right] \right) \triangleq R'_C \end{aligned} \quad (12)$$

where the summand in the second summation represents the first-order approximation to the logarithm of the denominator of (3) at the t th iteration, and

$$\Omega_k^{(t)} = \sum_{i=1, i \neq k}^K \mathbf{H}_k^{\text{BS}} \mathbf{Q}_i^{(t)} (\mathbf{H}_k^{\text{BS}})^H + \sum_{\ell=1}^L \mathbf{G}_k^\ell \mathbf{P}_\ell^{(t)} (\mathbf{G}_k^\ell)^H + \Phi_k^{\text{C}} \quad (13)$$

denotes the value of Ω_k at the t th iteration with $\{\mathbf{Q}_k\}$ and $\{\mathbf{P}_\ell\}$ given by $\{\mathbf{Q}_k^{(t)}\}$ and $\{\mathbf{P}_\ell^{(t)}\}$, respectively. The first-order approximation to R_{D} , denoted by R'_{D} , can be similarly formulated. While $R_{\text{C}} + R_{\text{D}}$ has been convexified through CCCP, the resultant objective in (11a) is still nonconvex due to the fractional form. Thus, we adopt the Dinkelbach method to deal with the nonconvex fractional form of (11a).

B. Dinkelbach Method

For notational convenience, let $U_1(\mathbf{Q}_k, \mathbf{P}_\ell) = R'_{\text{C}} + R'_{\text{D}}$ and $U_2(\mathbf{Q}_k, \mathbf{P}_\ell) = P_{\text{C}}^{\text{Total}} + P_{\text{D}}^{\text{Total}}$. Then, after approximating $R_{\text{C}} + R_{\text{D}}$ by $R'_{\text{C}} + R'_{\text{D}}$, problem (11) becomes

$$\max_{\{\mathbf{Q}_k\}, \{\mathbf{P}_\ell\}} \frac{U_1(\mathbf{Q}_k, \mathbf{P}_\ell)}{U_2(\mathbf{Q}_k, \mathbf{P}_\ell)} \quad (14a)$$

$$\text{s.t. (11b), (11c), (11d), (11e), (11f), (11g).} \quad (14b)$$

Define

$$\alpha \triangleq \frac{U_1(\mathbf{Q}_k, \mathbf{P}_\ell)}{U_2(\mathbf{Q}_k, \mathbf{P}_\ell)}. \quad (15)$$

To exploit the Dinkelbach method [15], [16], [21], consider the following theorem.

Theorem 1 *The maximal value of α in (15), denoted by α^* , is achieved if and only if*

$$\begin{aligned} \max_{\{\mathbf{Q}_k\}, \{\mathbf{P}_\ell\}} U_1(\mathbf{Q}_k, \mathbf{P}_\ell) - \alpha^* U_2(\mathbf{Q}_k, \mathbf{P}_\ell) \\ = U_1(\mathbf{Q}_k^*, \mathbf{P}_\ell^*) - \alpha^* U_2(\mathbf{Q}_k^*, \mathbf{P}_\ell^*) \\ = 0, \end{aligned} \quad (16)$$

where $(\mathbf{Q}_k^*, \mathbf{P}_\ell^*)$ are the optimal solution of (14) for $U_1(\mathbf{Q}_k, \mathbf{P}_\ell) \geq 0$ and $U_2(\mathbf{Q}_k, \mathbf{P}_\ell) > 0$.

Proof: See Appendix A. ■

Using the result in Theorem 1, we can equivalently reformulate (14) as the following optimization problem:

$$\max_{\{\mathbf{Q}_k\}, \{\mathbf{P}_\ell\}, \{\alpha\}} U_1(\mathbf{Q}_k, \mathbf{P}_\ell) - \alpha U_2(\mathbf{Q}_k, \mathbf{P}_\ell) \quad (17a)$$

$$\text{s.t. (11b), (11c), (11d), (11e), (11f), (11g).} \quad (17b)$$

Note that the joint optimization over \mathbf{Q}_k , \mathbf{P}_ℓ , and α in (17) is very difficult due to non-convexity. Fortunately, the problem will be jointly convex with respect to $(\mathbf{Q}_k, \mathbf{P}_\ell)$ when α is given. This property suggests a two-stage algorithm, as elaborated below. First, we determine α with a bisection algorithm. Then, with the given α , we solve problem (17) and obtain the optimal \mathbf{Q}_k and \mathbf{P}_ℓ . The bisection algorithm is terminated when the difference of α is small enough between

iterations. Finally, we adopt the Cholesky decomposition on \mathbf{Q}_k to obtain the optimal \mathbf{W}_k for all $k \in \mathcal{K}$. The overall procedure is detailed in Algorithm 1.

Algorithm 1 Algorithm to Solve Problem (17)

- 1: **Initialize:**
 - 2: Generate initial values for $t \leftarrow 0$
 - 3: $\mathbf{Q}_k^{(t)} = \widehat{\mathbf{Q}}_k^{(t)} (\widehat{\mathbf{Q}}_k^{(t)})^H$ for $k \in \mathcal{K}$ where $\widehat{\mathbf{Q}}_k^{(t)}$ is the random i.i.d. complex Gaussian random variables with zero mean and unit variance. Then, $\mathbf{Q}_k^{(t)} = \frac{\mathbf{Q}_k^{(t)}}{\|\widehat{\mathbf{Q}}_k^{(t)}\|^2}$.
 - 4: $\mathbf{P}_\ell^{(t)} = \widehat{\mathbf{P}}_\ell^{(t)} (\widehat{\mathbf{P}}_\ell^{(t)})^H$ for $\ell \in \mathcal{L}$ where $\widehat{\mathbf{P}}_\ell^{(t)}$ is the random i.i.d. complex Gaussian random variables with zero mean and unit variable. Then, $\mathbf{P}_\ell^{(t)} = \frac{\mathbf{P}_\ell^{(t)}}{\|\widehat{\mathbf{P}}_\ell^{(t)}\|^2}$.
 - 5: **repeat**
 - 6: Given an interval $[\alpha_{\text{max}}, \alpha_{\text{min}}]$, tolerance $\epsilon > 0$
 - 7: **while** $(\alpha_{\text{max}} - \alpha_{\text{min}}) > \epsilon$ **do**
 - 8: $\alpha = (\alpha_{\text{max}} + \alpha_{\text{min}})/2$
 - 9: Solve problem (17).
 - 10: **if** The above problem is feasible **then**
 - 11: $\alpha_{\text{min}} = \alpha$
 - 12: **else if** **then**
 - 13: $\alpha_{\text{max}} = \alpha$
 - 14: **end if**
 - 15: **end while**
 - 16: $t \leftarrow t + 1$
 - 17: Update: $\mathbf{Q}_k^{(t)} = \mathbf{Q}_k^*$ and $\mathbf{P}_\ell^{(t)} = \mathbf{P}_\ell^*$
 - 18: **until** Convergence
 - 19: Apply the Cholesky decomposition to \mathbf{Q}_k^* to find the precoder \mathbf{W}_k^* .
-

We next explore the convergence behavior of the proposed algorithm. If the objective function (17a) is strictly monotonically increasing, then the convergence characteristics of a CCCP plus Dinkelbach method can be guaranteed. This is established in the following theorem.

Theorem 2 *Suppose that problem (17) is feasible. Then, the objective function (17a) is strictly monotonically increasing with the algorithmic iterations in Algorithm 1 unless $\mathbf{Q}_k^{(t+1)} = \mathbf{Q}_k^{(t)}$ and $\mathbf{P}_\ell^{(t+1)} = \mathbf{P}_\ell^{(t)}$.*

Proof: See Appendix B. ■

V. SIMULATIONS RESULTS

In simulations, execution of Algorithm 1 entails a triple-nested loop. The outer loop is to remove the fractional form of the original nonlinear fractional problem for better tractability, the middle loop is CCCP for sequential convex approximation, and the inner loop is the interior point method for convex optimization.

We simulate an EH-enabled D2D underlaid MIMO cellular network with $K = 1$ CUE and $L = 3$ pairs of DUEs, as depicted in Fig. 2. The CUE and DUE transmitters are uniformly distributed in a 50×50 m² area. The distance between the DUE transmitter and the paired DUE receiver is

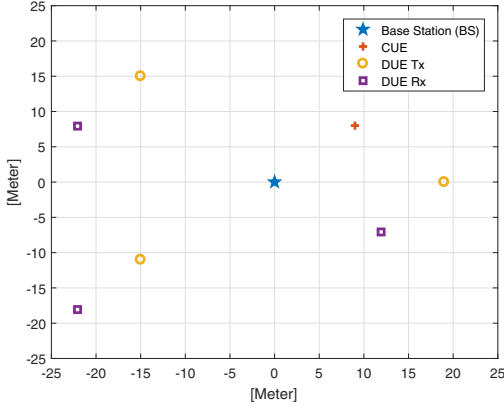


Fig. 2. Network topology with $K = 1$ and $L = 3$.

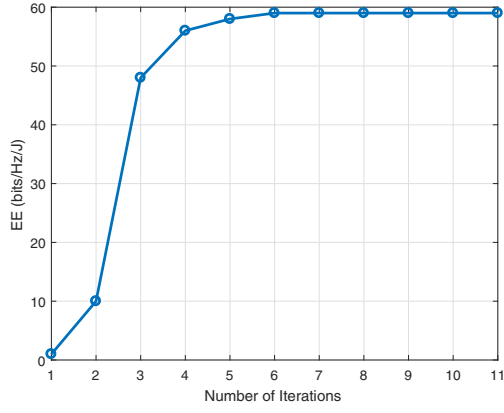


Fig. 3. Convergence behavior of the proposed algorithm, with $P_{\max}^C = 46$ dBm, $P_{\max}^D = 10$ dBm, $E_{\min}^C = E_{\min}^D = -20$ dBm, $K = 1$, and $L = 3$.

10 m. The channel is modeled as $(d)^{-3}\delta$, where d represents the distance in meters between the receiver and the transmitter, and $\delta \sim \mathcal{CN}(0,1)$ is the Rayleigh fading coefficient. We set the thermal noise variances $\sigma_k^2 = \sigma_\ell^2 = -70$ dBm, the variances of the circuit noises introduced at the information decoder $\tilde{\sigma}_k^2 = \tilde{\sigma}_\ell^2 = -50$ dBm, numbers of antennas $N_t^C = 4$, $N_t^D = 2$, $N_r = 2$, the maximum transmit power at the BS $P_{\max}^C = 46$ dBm, the maximum transmit power at each transmitting DUE $P_{\max}^D = 10$ dBm, the target harvested energy $E_{\min}^C = E_{\min}^D = -20$ dBm, the circuit power consumption at the BS $P_{\text{BS}}^{\text{cir}} = 3.1622$ mW, the circuit power consumption at the transmitter of the ℓ th DUE pair $P_{\ell}^{\text{cir}} = 1.9952$ mW [14], the power-splitting factor at all devices $\rho_k^C = \rho_\ell^D = \rho = 0.5, \forall k, \ell$, and the energy conversion efficiency $\xi_k^C = \xi_\ell^D = 1, \forall k, \ell$. The stopping threshold in the bisection method is given as 10^{-6} . All the results are obtained by averaging a sufficient number of matrix channel realizations.

Fig. 3 illustrates the convergence behavior of Algorithm 1. The result verifies Theorem 2 and shows that Algorithm 1

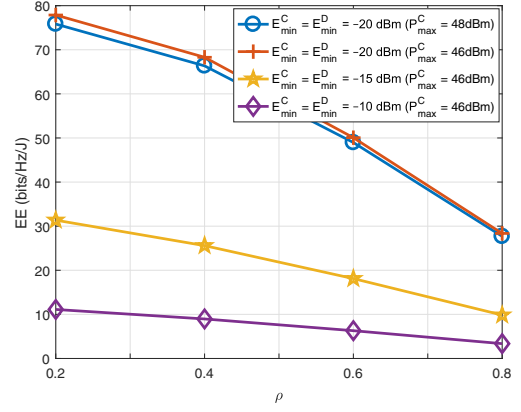


Fig. 4. EE vs. the power-splitting factor, with $P_{\max}^D = 10$ dBm, $K = 1$, and $L = 3$.

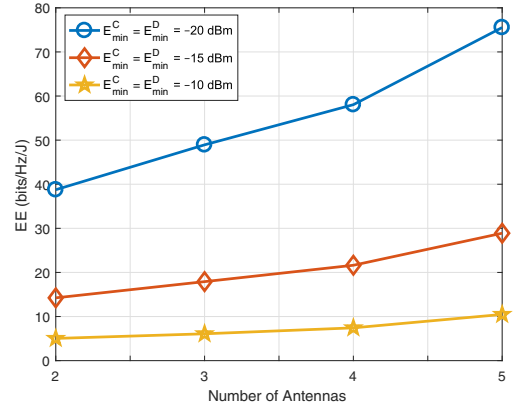


Fig. 5. EE vs. the number of antennas at the BS, with $P_{\max}^C = 46$ dBm, $P_{\max}^D = 10$ dBm, $K = 1$, and $L = 3$.

converges in few iterations.

Fig. 4 plots the EE vs. the power-splitting factor performance. The figure shows a monotonic decrease in the EE with an increasing power-splitting factor ρ . This is because, when ρ increases, more power is directed to information decoding and thus the system sum rate increases. However, when ρ increases, the amount of harvested energy decreases, and thus to meet the EH constraint higher transmit power is needed, resulting in higher total system power consumption. The overall effect is EE reduction. When P_{\max}^C increases or when $E_{\min}^C = E_{\min}^D$ increases, EE decreases for a given ρ . This is because meeting a higher EH demand requires more transmit power from the BS, which in turn reduces the system EE.

Fig. 5 plots the EE vs. the number of antennas at the BS performance. As can be seen, EE increases with an increasing number of antennas at the BS (assuming the same circuit power consumption). It is also observed here that when $E_{\min}^C = E_{\min}^D$ increases, EE decreases, as explained previously.

VI. CONCLUSION

In this paper, we have studied the EE maximization problem in EH-based D2D communication underlaid MIMO cellular networks. The objective was to find the optimal precoders at the BS and power allocation at the transmitting DUEs such that the system EE performance can be maximized under EH and transmit power constraints. The optimization problem was formulated as a nonlinear fractional programming problem. We approached this problem by using the CCCP and the Dinkelbach method. Numerical experiments demonstrated the performance of the proposed method, including the tradeoff between the network EE and the target harvested energy.

APPENDIX A PROOF OF THEOREM 1

First, we verify the necessary condition based on [21], [23]. For any feasible α , we have

$$\alpha^* = \frac{U_1(\mathbf{Q}_k^*, \mathbf{P}_\ell^*)}{U_2(\mathbf{Q}_k^*, \mathbf{P}_\ell^*)} \geq \frac{U_1(\mathbf{Q}_k, \mathbf{P}_\ell)}{U_2(\mathbf{Q}_k, \mathbf{P}_\ell)} \quad (18)$$

Rearranging (18) leads to

$$U_1(\mathbf{Q}_k^*, \mathbf{P}_\ell^*) - \alpha^* U_2(\mathbf{Q}_k^*, \mathbf{P}_\ell^*) = 0, \quad (19)$$

$$U_1(\mathbf{Q}_k, \mathbf{P}_\ell) - \alpha^* U_2(\mathbf{Q}_k, \mathbf{P}_\ell) \leq 0. \quad (20)$$

Thus, the maximum value of $U_1(\mathbf{Q}_k, \mathbf{P}_\ell) - \alpha^* U_2(\mathbf{Q}_k, \mathbf{P}_\ell)$ is 0, and is achieved by α^* , which is obtained by solving the EE maximization problem defined in (14). This completes the necessity proof.

To show sufficiency, suppose that $\{\widetilde{\mathbf{Q}}_k, \widetilde{\mathbf{P}}_\ell\}$ is the optimal solution to problem (14) which satisfies

$$U_1(\mathbf{Q}_k, \mathbf{P}_\ell) - \alpha^* U_2(\mathbf{Q}_k, \mathbf{P}_\ell) \leq U_1(\widetilde{\mathbf{Q}}_k, \widetilde{\mathbf{P}}_\ell) - \alpha^* U_2(\widetilde{\mathbf{Q}}_k, \widetilde{\mathbf{P}}_\ell) = 0. \quad (21)$$

By rearranging (21), we obtain

$$\alpha^* = \frac{U_1(\widetilde{\mathbf{Q}}_k, \widetilde{\mathbf{P}}_\ell)}{U_2(\widetilde{\mathbf{Q}}_k, \widetilde{\mathbf{P}}_\ell)} \geq \frac{U_1(\mathbf{Q}_k, \mathbf{P}_\ell)}{U_2(\mathbf{Q}_k, \mathbf{P}_\ell)}. \quad (22)$$

Hence, $\{\widetilde{\mathbf{Q}}_k, \widetilde{\mathbf{P}}_\ell\}$ are also the solution of the EE maximization problem defined in (14), i.e., $\{\widetilde{\mathbf{Q}}_k, \widetilde{\mathbf{P}}_\ell\} = \{\mathbf{Q}_k^*, \mathbf{P}_\ell^*\}$. This validates the sufficient condition.

APPENDIX B PROOF OF THEOREM 2

For notational convenience, let $\Lambda = [\mathbf{Q}_k, \mathbf{P}_\ell]$ and $\Lambda^{(t)} = [\mathbf{Q}_k^{(t)}, \mathbf{P}_\ell^{(t)}]$. Let $f(\Lambda)$ denote the objective function (17a), which can be rewritten as

$$f(\Lambda) = f_{\text{concave}}(\Lambda) + f_{\text{convex}}(\Lambda) \quad (23)$$

where

$$f_{\text{concave}}(\Lambda) \triangleq \sum_{k=1}^K \log_2 \left| \sum_{i=1}^K \mathbf{H}_k^{\text{BS}} \mathbf{Q}_i (\mathbf{H}_k^{\text{BS}})^H + \sum_{\ell=1}^L \mathbf{G}_k^\ell \mathbf{P}_\ell (\mathbf{G}_k^\ell)^H + \Phi_k^{\text{C}} \right| + \sum_{\ell=1}^L \log_2 \left| \sum_{j=1}^L \mathbf{H}_\ell^j \mathbf{P}_j (\mathbf{H}_\ell^j)^H + \sum_{k=1}^K \mathbf{G}_\ell^{\text{BS}} \mathbf{Q}_k (\mathbf{G}_\ell^{\text{BS}})^H + \Phi_\ell^{\text{D}} \right|, \quad (24)$$

and

$$f_{\text{convex}}(\Lambda) \triangleq - \sum_{k=1}^K \left(\log_2 |\Omega_k^{(t)}| + \frac{1}{\ln(2)} \text{Tr} \left[(\Omega_k^{(t)})^{-1} (\Omega_k - \Omega_k^{(t)}) \right] \right) - \sum_{\ell=1}^L \left(\log_2 |\Psi_\ell^{(t)}| + \frac{1}{\ln(2)} \text{Tr} \left[(\Psi_\ell^{(t)})^{-1} (\Psi_\ell - \Psi_\ell^{(t)}) \right] \right) - \alpha (P_{\text{C}}^{\text{Total}} + P_{\text{D}}^{\text{Total}}) \quad (25)$$

with

$$\Psi_\ell^{(t)} = \sum_{j \neq \ell}^L \mathbf{H}_\ell^j \mathbf{P}_j^{(t)} (\mathbf{H}_\ell^j)^H + \sum_{k=1}^K \mathbf{G}_\ell^{\text{BS}} \mathbf{Q}_k^{(t)} (\mathbf{G}_\ell^{\text{BS}})^H + \Phi_\ell^{\text{D}}. \quad (26)$$

Without loss of generality, we omit the affine function $\alpha (P_{\text{C}}^{\text{Total}} + P_{\text{D}}^{\text{Total}})$ in the following. When $\Lambda^{(t+1)} \neq \Lambda^{(t)}$, we have

$$\begin{aligned} f(\Lambda^{(t+1)}) &= f_{\text{concave}}(\Lambda^{(t+1)}) + f_{\text{convex}}(\Lambda^{(t+1)}) \\ &> f_{\text{concave}}(\Lambda^{(t+1)}) \\ &\quad + f_{\text{convex}}(\Lambda^{(t)}) + \nabla f_{\text{convex}}(\Lambda^{(t)}) (\Lambda^{(t+1)} - \Lambda^{(t)})^T \\ &\geq f_{\text{concave}}(\Lambda^{(t)}) - \nabla f_{\text{convex}}(\Lambda^{(t)}) (\Lambda^{(t+1)} - \Lambda^{(t)})^T \\ &\quad + f_{\text{convex}}(\Lambda^{(t)}) + \nabla f_{\text{convex}}(\Lambda^{(t)}) (\Lambda^{(t+1)} - \Lambda^{(t)})^T \\ &= f_{\text{concave}}(\Lambda^{(t)}) + f_{\text{convex}}(\Lambda^{(t)}) \\ &= f(\Lambda^{(t)}) \end{aligned} \quad (27)$$

where the first (strict) inequality uses the fact that the first-order Taylor approximation of a convex function is always a global underestimation of the function, and the second inequality follows from solving problem (17), with the objective (17a) being expressed as (23), at the t th iteration. This completes the proof.

REFERENCES

- [1] X. Lin, J. G. Andrews, A. Ghosh, and R. Ratasuk, "An overview of 3GPP device-to-device proximity services," *IEEE Commun Mag.*, vol. 52, no. 4, pp. 40–48, Apr. 2014.
- [2] G. Fodor *et al.*, "An overview of device-to-device communications technology components in METIS," *IEEE Access*, vol. 4, pp. 3288–3299, July 2016.
- [3] H. Gao, M. Wang, and T. Lv, "Energy efficiency and spectrum efficiency tradeoff in the D2D-enabled HetNet," *IEEE Trans. Veh. Technol.*, vol. 66, no. 11, pp. 10 583–10 587, Nov. 2017.
- [4] Z. Zhou, K. Ota, M. Dong, and C. Xu, "Energy efficient matching for resource allocation in D2D enabled cellular networks," *IEEE Trans. Veh. Technol.*, vol. 66, no. 6, pp. 5256–5268, June 2017.

- [5] D. Feng, G. Yu, C. Xiong, Y. Y. Wu, G. Y. Li, G. Feng, and S. Li, "Mode switching for energy-efficient device-to-device communications in cellular networks," *IEEE Trans. Wireless Commun.*, vol. 14, no. 12, pp. 6993–7003, Dec. 2015.
- [6] T. D. Hoang, L. B. Le, and T. Le-Ngoc, "Energy efficient resource allocation for D2D communication in cellular networks," *IEEE Trans. Veh. Technol.*, vol. 65, no. 9, pp. 6972–6986, Sep. 2016.
- [7] S. Ulukus, A. Yener, E. Erkip, O. Simeone, M. Zorzi, P. Grover, and K. Huang, "Energy harvesting wireless communications: A review of recent advances," *IEEE J. Sel. Areas. Commun.*, vol. 33, no. 3, pp. 360–381, Mar. 2015.
- [8] Y. Zeng, B. Clerckx, and R. Zhang, "Communications and signals design for wireless power transmission," *IEEE Trans. Commun.*, vol. 65, no. 5, pp. 2264–2290, May 2017.
- [9] S. Gupta, R. Zhang, and L. Hanzo, "Energy harvesting aided device-to-device communication underlying the cellular downlink," *IEEE Access*, vol. 5, pp. 7405–7413, Jun. 2017.
- [10] M.-L. Ku and J.-W. Lai, "Joint beamforming and resource allocation for wireless-powered device-to-device communications in cellular networks," *IEEE Trans. Wireless Commun.*, vol. 16, no. 11, pp. 7290–7304, Nov 2017.
- [11] R. Atat, L. Liu, N. Mastrorade, and Y. Yi, "Energy harvesting-based D2D-assisted machine-type communications," *IEEE Trans. Commun.*, vol. 65, no. 3, pp. 1289–1302, Mar. 2017.
- [12] Z. Zhou, C. Gao, C. Xu, T. Chen, D. Zhang, and S. Mumtaz, "Energy efficient stable matching for resource allocation in energy harvesting-based device-to-device communications," *IEEE Access*, vol. 5, pp. 15 184–15 196, Aug. 2017.
- [13] C.-H. Lee, R. Y. Chang, C.-T. Lin, and S.-M. Cheng, "Sum-rate maximization for energy harvesting-aided D2D communications underlaid cellular networks," in *Proc. IEEE Personal, Indoor, and Mobile Radio Communications (PIMRC)*, Oct. 2017.
- [14] D. Nguyen, L.-N. Tran, P. Pirinen, and M. Latva-aho, "Precoding for full duplex multiuser MIMO systems: Spectral and energy efficiency maximization," *IEEE Trans. Signal Process.*, vol. 61, no. 16, pp. 4038–4050, Aug. 2013.
- [15] C. Isheden, Z. Chong, E. Jorswieck, and G. Fettweis, "Framework for link-level energy efficiency optimization with informed transmitter," *IEEE Trans. Wireless Commun.*, vol. 11, no. 8, pp. 2946–2957, Aug. 2012.
- [16] K. Shen and W. Yu, "Fractional programming for communication systems-part I: Power control and beamforming," *IEEE Trans. Signal Process.*, vol. 66, no. 10, pp. 2616–2630, May 2018.
- [17] M. Grant and S. Boyd. (2009, June) CVX: Matlab software for disciplined convex programming. [Online]. Available: <http://cvxr.com/cvx/>
- [18] Z.-Q. Luo and S. Zhang, "Dynamic spectrum management: Complexity and duality," *IEEE J. Sel. Topics Signal Process.*, vol. 2, no. 1, pp. 57–73, Feb. 2008.
- [19] Y. F. Liu, Y. H. Dai, and Z. Q. Luo, "Coordinated beamforming for MISO interference channel: Complexity analysis and efficient algorithms," *IEEE Trans. Signal Processing*, vol. 59, no. 3, pp. 1142–1157, Mar. 2011.
- [20] A. L. Yuille and A. Rangarajan, "The concave-convex procedure (CCCP)," in *Proc. Adv. Neural Inf. Process. Syst.*, pp. 1033–1040, 2001.
- [21] W. Dinkelbach, "On nonlinear fractional programming," *Bulletin of the Australian Mathematical Society*, vol. 13, pp. 492–498, Mar. 1967.
- [22] Y. Sun, P. Babu, and D. P. Palomar, "Majorization-minimization algorithms in signal processing, communications, and machine learning," *IEEE Trans. Signal Process.*, vol. 65, no. 3, pp. 794–816, Feb 2017.
- [23] Z. Zhou, M. Dong, K. Ota, J. Wu, and T. Sato, "Energy efficiency and spectral efficiency tradeoff in device-to-device (D2D) communications," *IEEE Wireless Commun. Lett.*, vol. 3, no. 5, pp. 485–488, Oct. 2014.